ECOLOGY LETTERS

Ecology Letters, (2017) **20**: 1566–1575 doi: 10.1111/ele.12866

LETTER

High mortality and enhanced recovery: modelling the countervailing effects of disturbance on population dynamics

Laura E. McMullen,[1] Patrick De Leenheer,[1,2] Jonathan D. Tonkin[1] and David A. Lytle[1]*

[1]*Department of Integrative Biology, Oregon State University, 3029 Cordley Hall, Corvallis, OR 97331, USA*
[2]*Department of Mathematics, Oregon State University, 368 Kidder Hall, Corvallis, OR 97331, USA*

**Correspondence: E-mail: lytleda@oregonstate.edu*

Abstract

Disturbances cause high mortality in populations while simultaneously enhancing population growth by improving habitats. These countervailing effects make it difficult to predict population dynamics following disturbance events. To address this challenge, we derived a novel form of the logistic growth equation that permits time-varying carrying capacity and growth rate. We combined this equation with concepts drawn from disturbance ecology to create a general model for population dynamics in disturbance-prone systems. A river flooding example using three insect species (a fast life-cycle mayfly, a slow life-cycle dragonfly and an ostracod) found optimal trade-offs between disturbance frequency vs. magnitude and a close fit to empirical data in 62% of cases. A savanna fire analysis identified fire frequencies of 3–4 years that maximised population size of a perennial grass. The model shows promise for predicting population dynamics after multiple disturbance events and for management of river flows and fire regimes.

Keywords

Disturbance ecology, invertebrate, population dynamics, resilience, resistance.

Ecology Letters (2017) **20**: 1566–1575

INTRODUCTION

Understanding the effects of disturbance on population dynamics is critical for predicting species abundance and persistence over time. On the one hand, disturbances such as floods, fires, and extreme rainfall events impose high mortality via movement of substrates, destruction of habitat, and direct trauma. On the other hand, disturbances may positively affect population growth by regenerating physical habitats, enhancing food resources, and maintaining physical linkages between adjacent habitats such as rivers and their floodplains (Junk *et al*. 1989; Power *et al*. 1996; Effenberger *et al*. 2006). These countervailing disturbance effects – immediate mortality vs. enhanced population growth – create complex population dynamics that are challenging to predict. Adding to these complexities, successional processes can ameliorate the effects of disturbances over time. For example, disturbances such as grassland fires or riverine floods can provide fresh substrates for recruitment, increased nutrients, and removal of nuisance algae or necromass, but these benefits eventually diminish over time.

Population dynamic models are essential for the management and conservation of many species, as well as for understanding their basic ecology and evolution. Prescribed fires are used to manage both vegetative and animal communities in terrestrial habitats (Pyke *et al*. 2010), and riverine flow prescriptions are used to manage populations of aquatic species in dammed rivers (Richter *et al*. 2006; Poff *et al*. 2010). Population models could, for example, help dam managers choose between allocating a fixed volume of water to more frequent, smaller flow events vs. fewer, larger releases based on the population-level outcomes of each scenario (Richter *et al*. 2003). Population dynamics also drive evolutionary processes, and disturbance-mediated selective pressures may influence the evolution of life histories, behaviours and morphologies that allow individuals to escape or withstand disturbances (Holomuzki & Biggs 2000; Lytle 2001; Lytle & Poff 2004; Lytle *et al*. 2007). A strong quantitative linkage between disturbance events and their population dynamic consequences could be used to examine fundamental ecological questions, such as the relationship between resistance (the ability of an organism to withstand disturbance) and resilience (the ability of a population to recover following disturbance) (Halpern 1988; Grimm & Fisher 1989; Nimmo *et al*. 2015). Thus, a disturbance population model would provide a foundation for basic eco-evolutionary research as well as the conservation of ecosystems.

Our goal is to first derive a basic disturbance model that captures the fundamental dynamics of population growth, disturbance mortality and disturbance-mediated changes to carrying capacity in the context of logistic population growth. Our modelling approach is deliberately abiotic, in that we focus on how multiple species respond autecologically to environmental disturbance events. This interaction neutral approach allows us to examine how the vital rates of individual species (growth rate, fecundity and survivorship) interact with disturbance regimes to produce population dynamics without relying on assumptions about among-species biotic interactions (Lytle *et al*. 2017). The mechanistic approach we take also allows a direct mapping between individual disturbance events and their population-level consequences, which allows the model to accommodate non-stationary disturbance regimes such as shifts due to climate change (Shenton *et al*. 2012; Yen *et al*. 2013; Bond *et al*. 2015; Lytle *et al*. 2017). We begin with the general framework of logistic population growth because of its economy of assumptions (initial population size, growth rate and carrying capacity) and then we relax assumptions to accommodate complex disturbance regimes that vary in magnitude, frequency and timing. To our knowledge, this is the first time that a logistic population

growth model has been applied to understand time-varying phenomena such as disturbance dynamics.

We use riverine flooding and savanna fire as case studies to explore the model. For the river example, we calibrate the model for three contrasting life histories that span a representative range of riverine aquatic invertebrates: a fast life-cycle mayfly that experiences high flood mortality but recovers rapidly post-disturbance; a slow life-cycle dragonfly that requires occasional flood events to provide cleanly scoured habitat and an ostracod seed shrimp that reproduces rapidly but favours non-flooding, still-water habitats. For the fire example, we calibrate the model based on the life history of a perennial grass inhabiting tropical savannas. We also use the model to explore the relationship between resistance and resilience to disturbance.

METHODS

Model description

The standard logistic equation expresses growth rate for a population of size N at time t, assuming a constant carrying capacity K and a constant maximal *per-capita* growth rate r:

$$\frac{dN}{dt}(t) = rN(t)\left(1 - \frac{N(t)}{K}\right), N(t_0) = N_0 \quad (1)$$

This equation can be solved for population size $N(t)$ given an initial population size N_0.

A more general form of this equation assumes that instead of constants, the carrying capacity and maximal per-capita growth rate can fluctuate in time. Denoting these by $K(t)$ and $r(t)$, respectively, the equation becomes:

$$\frac{dN}{dt}(t) = r(t)N(t)\left(1 - \frac{N(t)}{K(t)}\right), N(t_0) = N_0 \quad (2)$$

Under rather general assumptions about the time-dependence of both $r(t)$ and $K(t)$, we present a novel time-varying solution for $N(t)$ (details in Appendix S1):

$$N(t) = \frac{\left(e^{\int_{t_0}^{t} r(\tau)d\tau}\right)N_0}{\left(\int_{t_0}^{t} \frac{r(\tau)}{K(\tau)} e^{\int_{t_0}^{\tau} r(s)ds} d\tau\right)N_0 + 1} \quad (3)$$

Equation 3 provides a general framework for incorporating biological situations where r and K might vary through time due to external environmental forces such as changes in habitat quality, abrupt disturbances, or changes in the species' biology. N_0 is population size immediately following a disturbance event, and τ and s are integration variables which will disappear from the expression after the integrals have been evaluated, leading to a function that depends only on time t. While we examine some specific cases of eqn 3 below, this novel derivation creates new opportunities for the study of population dynamics and deserves a more thorough exploration of its general dynamics elsewhere.

To explore the dynamics of time-varying changes in carrying capacity, we make the simplifying assumption that r is constant, so eqn 3 reduces to

$$N(t) = \frac{e^{r(t-t_0)}N_0}{\left(\int_{t_0}^{t} \frac{e^{r(\tau-t_0)}r}{K(\tau)} d\tau\right)N_0 + 1} \quad (4)$$

Equation 4 describes situations where external factors such as habitat quality might change through time, allowing K to fluctuate up or down. We are interested in the situation where pulse disturbance events cause mortality in populations while simultaneously changing K by either enhancing or reducing habitat quality. The general framework can accommodate disturbance such as flooding, fire, pest outbreaks, or drought events. We allow disturbance mortality to occur in proportion to the disturbance's magnitude Q according to a negative exponential function:

$$N_0 = N_z e^{-hQ} \quad (5)$$

where h is a shape parameter describing the relationship between disturbance magnitude and disturbance-induced mortality, and N_z is population size immediately prior to the disturbance event. A negative exponential form arises when individuals in the population have the same per-capita risk of mortality. Larger values of Q imply more exposure to mortality risk, although there is always a finite possibility of survival even for large Q. Equation 5 was chosen to be a continuous function here, but a threshold function could be used in cases where disturbance events below a minimum magnitude do not cause mortality.

We include alterations to the species' habitat (either improvement or degradation) by assuming that a disturbance of magnitude Q will alter carrying capacity immediately post-disturbance according to:

$$K_0 = K_{pre} + (K_d - K_{pre})Q_f \quad (6)$$

where K_d is the carrying capacity limit following a large disturbance event and K_{pre} is carrying capacity immediately prior to the event. K_0 will be larger than K_{pre} for species whose habitat is improved by disturbances and smaller than K_{pre} for species whose habitat is degraded by disturbances. Q_f is a function that determines the shape of the relationship between disturbance magnitude and carrying capacity. In the simple case where larger disturbances have a larger effect on K_0, Q_f can be defined as:

$$Q_f = \begin{cases} 0 & \text{if } Q < Q_{min} \\ \frac{Q - Q_{min}}{a + (Q - Q_{min})} & \text{if } Q \geq Q_{min} \end{cases} \quad (7)$$

where Q_{min} is the minimum event magnitude that can be considered a disturbance, and a is a positive constant. Note that Q_f takes values in the interval [0, 1] for all possible values of the disturbance magnitude Q, and that Q_f increases towards 1 as Q approaches infinity. In the case of flooding disturbances, Q_{min} could be the minimum river discharge volume required to cause movement of substrates on the river bottom. The parameter a is the half-saturation constant, which determines the magnitude at which a disturbance event causes an addition to or subtraction from the pre-disturbance carrying capacity of half the difference between the pre-disturbance carrying capacity and K_d.

We assume that over time, successional processes in the habitat will eventually return carrying capacity to some pre-disturbance baseline value, K_b. We include this successional process by assuming that in the absence of more disturbances,

carrying capacity eventually reverts to K_b according to:

$$K(\tau) = K_b + (K_0 - K_b)e^{-g\tau} \quad (8)$$

The shape parameter g describes how rapidly carrying capacity returns to pre-disturbance levels. For the parameterisations we explore below, values of g near 0.01 allow carrying capacity to approach pre-disturbance levels within about a year following a large disturbance. The exponential shape of eqn 8 causes disturbance effects on carrying capacity to start diminishing immediately after the disturbance event and then gradually disappear as $K(\tau)$ approaches K_b. This is a convenient shape that has desirable properties (few parameters and smooth convergence), but other forms could be used if post-disturbance successional processes are well understood. Equation 8 is concave down when disturbances increase carrying capacity ($K_0 > K_b$) and concave up when disturbances decrease carrying capacity ($K_0 < K_b$).

The equations above can be used to study the effects of multiple, sequential disturbance events on carrying capacity and population size. When modelling sequential disturbances, we must keep track of the reduction in population size due to mortality and the change in carrying capacity due to successive disturbances. The pre-flood values N_z and K_{pre} can be calculated by evaluating eqns 4 and 8 at each specific flood time. The post-flood values N_0 and K_0 can then be calculated by evaluating eqns 5 and 6. These post-flood values can then re-initialise the population model in eqn 4, and the carrying capacity model in eqn 8, until the next disturbance occurs. A summary of descriptions and values for model parameters and values is found in Table 1.

Model performance

To explore model dynamics, we parameterised the model for three aquatic invertebrate taxa that span a diversity of life-cycle types. Intrinsic rates of population increase were estimated using a modified life-table approach with values obtained from the literature (Appendix S2). Table 1 describes the symbols used for parameters and variables in the model, their units, and default values used for the three target taxa. Modelling was implemented in Mathematica 10.2 (Wolfram Research 2015) and R (R Core Team 2015).

Fast life-cycle, flood-adapted species were represented by the mayfly *Fallceon quilleri* (Ephemeroptera: Baetidae), which can develop from egg to adult stage in as few as 7 days in Arizona, USA (Gray 1981). This species reproduces continuously in warm-climate streams and recolonises post-flood from upstream drift as well as from ovipositing aerial adults (Gray & Fisher 1981; Poff *et al*. 2006). In desert rivers, mayflies such as *Fallceon* benefit from flood-generated riffles and nutrient pulses that promote algal growth, so to reflect a strong positive flood enhancement we set the maximum possible carrying capacity (K_d) to 100 (a maximum population size of 100 allows us to interpret population size as a percentage) and the lowest possible carrying capacity (K_b) to 40 (absence of flooding limits populations to 40% of maximum possible). Carrying capacity after flood enhancements was assumed to diminish during succession, due to depletion of nutrient pulses and alteration of riffle habitats by encroaching riparian vegetation (Andersen & Shafroth 2010). Slow life-cycle, flood-adapted species were represented by the sanddragon dragonfly *Progomphus borealis* (Odonata: Gomphidae). Sanddragon larvae are large-bodied predators, and thus have a slower population growth rate compared to other aquatic invertebrates such as mayflies (Table 1). Sanddragons also possess behaviours for surviving flood displacement (Poff *et al*. 2006; Lytle *et al*. 2008), and this was included in the model by using a lower flood mortality rate (Table 1). This species is suited to open, sandy river channels that are created by flooding ($K_d = 100$ and $K_b = 40$ to reflect a positive flood enhancement). Species poorly adapted to flooding were represented by ostracod seed shrimp (Crustacea: Ostracoda). Ostracods are

Table 1 Model parameters and variables for flooding scenarios with default values for target taxa.

Symbol	Description	Units	Default values		
			Mayfly	Dragonfly	Ostracod
t	Time	Days			
N_t	Population size at time t	Individuals			
N_z	Population size pre-disturbance	Individuals			
N_0	Population size post-disturbance	Individuals			
K	Realised carrying capacity*	Individuals	40	40	100
K_d	Carrying capacity limit following strong disturbance	Individuals	100	100	40
K_b	Carrying capacity baseline when disturbances are absent	Individuals	40	40	100
K_0	Immediate post-disturbance carrying capacity	Individuals			
K_{pre}	Immediate pre-disturbance carrying capacity	Individuals			
r	Intrinsic rate of population increase	Individuals·day^{-1}	0.23	0.08	0.16
Q	Peak disturbance magnitude	m^3·s^{-1}			
Q_f	Function that determines disturbance–magnitude/carrying capacity relationship				
Q_{min}	Minimum event magnitude that can be considered a disturbance	m^3·s^{-1}	5	5	5
a	Half-saturation constant		100	100	100
h	Strength of disturbance–mortality relationship		0.02	0.01	0.05
g	Rate that K returns to pre-disturbance level		0.01	0.01	0.01

Note All parameters with units of individuals were re-scaled to a maximum of 100.
*K was set at the non-flood carrying capacity prior to the first flood event, but generally it changes as a function of flood magnitude and time.

filter feeders that prefer slow-water habitats and can reach high numbers in rivers with large amounts of established edge vegetation or beaver dam impoundments (Shafroth *et al.* 2010). Because floods reduce both of these preferred habitats, we assumed that floods have a strong negative effect on habitat quality (K_d = 40 and K_b = 100). We calculated a medium population growth rate and assumed a high mortality from flooding due to their limited swimming and crawling abilities, and apparent lack of flood-related survival behaviours (Table 1, Poff *et al.* 2006).

We examined population dynamics of the three target taxa after a single disturbance event and also after multiple disturbance events with flood magnitudes ranging from 1 to 1000 m^3 s^{-1} and flood frequencies of 1–10 floods per season, with floods occurring 5 days apart. We modelled how allocating a specified volume of water across a range of flood events (from 1 to 10 floods) affected population dynamics. This 'cumulative flood magnitude' is useful for understanding how population dynamics are differentially affected by multiple small disturbance events as opposed to fewer large events.

We also examined the sensitivity of population recovery (using eqn 4) to changes in the values of r (intrinsic rate of population increase) and h (strength of flood–mortality relationship). These parameters can be interpreted as measures of resilience (the ability of a population to recover from a disturbance) and resistance (the ability to withstand disturbance; in this case h represents inverse resistance) to disturbance.

Comparison with empirical estimates

We compared model predictions to observed population sizes of the three target taxa groups after three prescribed flood events on the Bill Williams River, AZ, USA. Methods for these experimental flow releases are described in Shafroth *et al.* (2010). We calibrated the model for predictions based on peak magnitudes of the prescribed floods at a U.S. Geological Survey discharge gauge (USGS gauge #9426000), the time post-flood that invertebrate sampling occurred and the observed relative population sizes at the study sites prior to the flood event. Population sizes were measured at three points along the river: Alamo Dam (0 km downstream of gauge), Rankin Ranch (18 km below gauge) and Mineral Wash (48 km below gauge). We relativised population sizes and variances according to the mean of the top three values for site abundance obtained over the project duration.

Application to savanna fire ecology

To explore the generality of our approach, we applied the model to disturbance from fire in tropical grasslands. We parameterised the model based on the life cycle of *Andropogon semiberbis*, a perennial grass that occurs in seasonal savannas in tropical South America (Silva & Castro 1989; Silva *et al.* 1990, 1991), living up to 8 years and reaching sexual maturity at 2 (Franco & Silvertown 2004). While prone to both natural and anthropogenic fire mortality at the seedling stage, *A. semiberbis* is adapted to fire due to its ability to withstand fire in mature stage classes. We sourced values of fire-specific mortality from seedling survivorship experiments reported in Silva *et al.* (1989), and corrected to a single population-wide value that accounts for low mortality in adults (i.e. divided by 3; m = 0.26). We employed a shape parameter (g) of 0.02 that ensured K returned to approximately 50% of its maximum value after 3 years (K ranged between 0 and 100). We sourced the intrinsic rate of population increase (r) from Silva *et al.* (1991), representing the realised r under fire regimes (0.2251). We varied fire return interval ($frequency^{-1}$) from annual to every 20 years, and assumed that fire magnitude remained constant across events. We forecasted population abundance for 50 years to ensure population cycles had stabilised.

RESULTS

General model performance

Overall, our implementation of the flooding example produced many of the population dynamic patterns that are typical of species inhabiting flood-prone rivers, although individual responses varied substantially across life-history types. Fig. 1 shows population response surfaces for the three aquatic invertebrates after a single-flood event at different values of Q. For most values of Q, population size of mayflies rose sharply as the population recovered post-flood, but eventually began to decline as beneficial flood enhancements diminished over time. For mayflies, the optimal balance between flood mortality and flood enhancements occurred at Q = 298 cms and t = 47 days, although the population never exceeded 68% of the maximum expected population size for any Q–t combination. A similar pattern was evident for dragonflies, although slower population growth rates coupled with lower flood mortality produced a different optimum (N_t = 60% at Q = 236 cms, t = 60 days). The low N_t values emphasise that at least for these two species, a single-flood event is not sufficient to boost a population to the theoretical maximum attainable size under the parameterised values. In contrast to the flood-adapted species, ostracod populations remained at 100% of their maximum population size when no flood occurred (Q = 0) but experienced a sharp decline even for small floods, although population recovery was usually evident between 150 and 200 days.

Resistance and resilience

Exploration of r–h parameter space revealed several notable features about the relationship between resistance and resilience under this model (Fig. 2). First, there was a sharp jump from parameter combinations that allowed rapid population recovery over short timescales compared to parameter combinations that did not. Within a relatively narrow parameter space, a small change in r or h created a large shift in potential population recovery after flood events – evidence for a threshold effect. Second, the surface on either side of the threshold was a relatively flat plateau, indicating the existence of many r-h parameter combinations that led to either strong or weak population response to disturbance. Parameter combinations on the surface of each plateau were numerically similar, in that they resulted in the nearly the same population sizes.

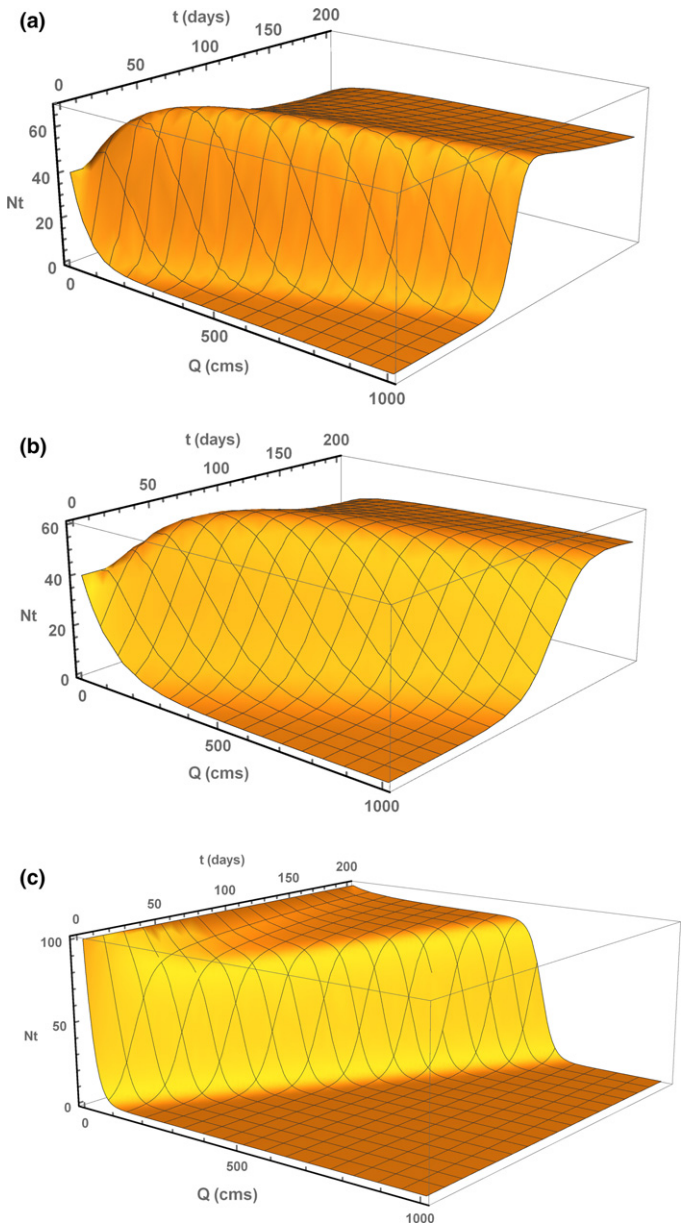

Figure 1 Flood–population response surfaces for three taxa with contrasting life histories after a single-flood event: (a) mayfly (*Fallceon quilleri*), (b) dragonfly (*Progomphus borealis*) and (c) ostracods (Ostracoda). Relative population size (N_t) vs. flood magnitude (Q) and time since flood event (t).

Multiple sequential disturbances

The modelled population-level consequences of multiple, sequential floods varied across taxa. Mayflies responded most favourably to floods, while dragonfly populations were the most resistant to disturbance. Ostracods were susceptible to large, sequential flood events with no evident recovery at 200 days following two sequential flood events. Differences were the most pronounced immediately following the series of disturbance events (20 days graphs in Fig. 3). These differences became less pronounced as time since the disturbance events increased (100 days graphs in Fig. 3).

Mayflies experienced the greatest population increases after multiple mid-sized flood events. High population sizes were never reached after a single flood no matter the magnitude, indicating that mayfly populations likely respond positively to sequences of mid-sized, more frequent events. Maximum population sizes occurred 20 days after 10 small floods of 400 cms magnitude. At 100 days post-disturbance, most of the benefits of flood disturbance had vanished, and population sizes had returned to baseline pre-disturbance values. Dragonflies responded positively to flooding on slower time scales, with the greatest population sizes occurring 100 days following any particular flooding sequence. Maximum population sizes occurred 100 days following 8–10 smaller floods of 400–700 cms cumulative magnitude. Thus, the slower growth dynamics of dragonflies caused flooding benefits to be realised much later in time than with mayflies. Ostracods numbers were maximised following no floods or very small floods. Even 100 days post-disturbance, ostracod populations were negatively impacted under all but the most benign flood scenarios. Ostracods populations were reduced the most severely by fewer, larger flood events.

Empirical model test

Overall, model predictions of relative population size fell within the 95% confidence intervals for observed population sizes 62% of the time (Table 2). The model differed in success at predicting relative population sizes among sampling sites on the river. The proportion of times that model predictions fell within the 95% confidence intervals of the observed population sizes at Rankin Ranch was only 53%, while it was 67% at both Mineral Wash and Alamo. There were also taxonomic differences in success of the model at predicting relative population sizes. The model was most successful at predicting relative population sizes for dragonflies, where predictions fell within the 95% confidence intervals 67% of the time. The model was least successful for mayflies (56% of the time). Model success also differed among years. Model predictions fell within the 95% confidence intervals of the observed population sizes 75% of the time in 2006 and 2007 but only 50% of the time in 2008.

Savanna fire frequency

Population cycles of savanna grass fluctuated according to the specified fire frequency, but reached the highest average population size at fire return intervals of 3 to 4 years (Fig. 4). A fire return interval of 1 year led to the population declining to zero, and above this populations maintained a stable cycle of population growth and decline attributable to either fire-induced mortality or carrying capacity decline. Fire mortality was the dominant cause of low population size for return intervals below 4 years, whereas carrying capacity became more important in scenarios with longer fire return intervals.

DISCUSSION

The disturbance model we have presented unifies basic logistic population growth with fundamental concepts drawn from

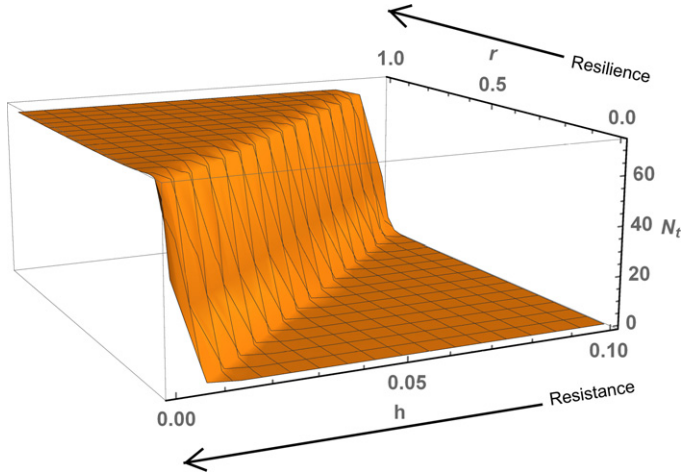

Figure 2 Plot of population size 50 days after a flood for a species whose habitat is enhanced by floods at different combinations of r and h. r is interpreted as a measure of resilience, and h as an inverse measure of resistance (lower h denotes greater resistance). There is a resistance–resilience threshold beyond which the trait combination allows, or disallows, timely recovery from flooding. $K_d = 100$; $K_b = 40$; $Q = 500$; $t = 50$; $g = 0.01$; $N_Z = 40$.

disturbance ecology. The model can be parameterised for any pulse disturbance (floods, fires and landslides) and, in principle, any species. The required information is an estimate of the species' intrinsic rate of population increase, expected mortality from disturbance and knowledge of how disturbances would alter habitat in relation to the species' preference. In the model, disturbances affect two key variables related to logistic population growth, initial population size (N_0) and carrying capacity (K). To our knowledge, this is the first model to combine logistic growth models with general disturbance ecology. Stage-specific population models have been used to predict the effect of flooding on riparian plants (Lytle & Merritt 2004; Smith *et al.* 2005; Elderd & Doak 2006; Schleuning *et al.* 2008), spatially explicit individual-based models have been used to examine effects disturbance on demographic rates and habitats (Elderd & Nott 2007; Keith *et al.* 2008) and other models have predicted effects of disturbances such as fires at the community level while still considering effects at the species level (He & Mladenoff 1999; Russell *et al.* 2009). Because population sizes and carrying capacities were represented in our model by scaling values to 100, the model results can be applied to any system as a percentage of the carrying capacity for a specific area of river habitat.

Our logistic disturbance model focuses on the abiotic effects of disturbances on population dynamics. Although biotic interactions between species certainly play a role in population dynamics (Wootton *et al.* 1996; Marks *et al.* 2000), it may not always be necessary to include these effects when considering abiotically dominated ecosystems such as flood-prone rivers or fire-prone savannas (Moyle & Light 1996; Marchetti & Moyle 2001; Lepori & Hjerdt 2006; Hoffman *et al.* 2009). In principle, the single-species models presented here could be linked to examine biotic interactions and to predict community dynamics, as with Lytle *et al.* (2017). However, the abiotically focused approach allows us to isolate the extent to which abiotic factors alone influence population dynamics (Death 2010), and the model can be used as a null that asks whether disturbance effects alone are sufficient for describing observed population dynamics in a system (Lytle & Merritt 2004; Lytle *et al.* 2017).

Aquatic taxa differed with respect to the size of a single flood that was most beneficial to their population levels, with smaller floods being more beneficial to dragonflies and mid-sized floods more beneficial to mayflies. Factors other than flood-induced mortality rates, such as flood alteration of habitat and differences in population life histories, appear to contribute to these results, highlighting the importance of incorporating these dynamics into modelling approaches. Not surprisingly, populations with faster growth rates such as mayflies reached maximum numbers after flood events more quickly than those with slower growth rates, such as dragonflies. Thus, it is important to consider the time scale of the species' population dynamics with respect to the time scale of disturbance dynamics (Townsend & Hildrew 1994; Tonkin *et al.* 2017).

The single-flood version of the model never allowed population levels to reach greater than 68% of maximum population size when looking at floods with magnitudes up to 1000 cms, suggesting that single-flood events may not produce enough habitat enhancement to allow populations to reach maximum levels. Also, single-flood events that might produce large enough enhancements to habitat often simultaneously produce great mortality, which hinders population recovery. Our modelling approach allows a close examination of this tradeoff between flood mortality and habitat enhancement, and the multi-disturbance version allows us to optimise population sizes across a wide distribution of disturbance frequencies and magnitudes.

Under the multi-flood model scenarios, populations eventually converged on similar relative abundances, regardless of the previous floods magnitudes (Fig. 3). This pattern was more evident for fast life-cycle, flood-adapted species (mayflies) than for species which are susceptible to flood events (ostracods). Mayflies were the least sensitive to differences in flood magnitude in the long run, while ostracods were the most sensitive. For ostracods, there was a sharp drop within the cumulative flood magnitude–number of floods relationship, where certain combinations of floods (primarily large, less frequent floods) did not allow populations to recover after 100 days, while other combinations (smaller, more frequent floods) allowed populations to recover to levels near carrying capacity (Fig. 3). For poorly flood-adapted taxa such as ostracods, multiple smaller floods may have a lesser effect on abundances than fewer, larger floods. Overall, our model showed that many small disturbances are not always equivalent to one or a few larger events in relation to aquatic population dynamics, and that the optimum allocation of disturbance magnitude vs. frequency varies across taxa.

Our comparison of flooding model predictions to observed data found that about two-thirds of the time, the model prediction fell within the 95% confidence interval of empirical data. In every case, the model predicted a higher abundance than what was observed from field data. The model was most successful at predicting post-flood relative population size for

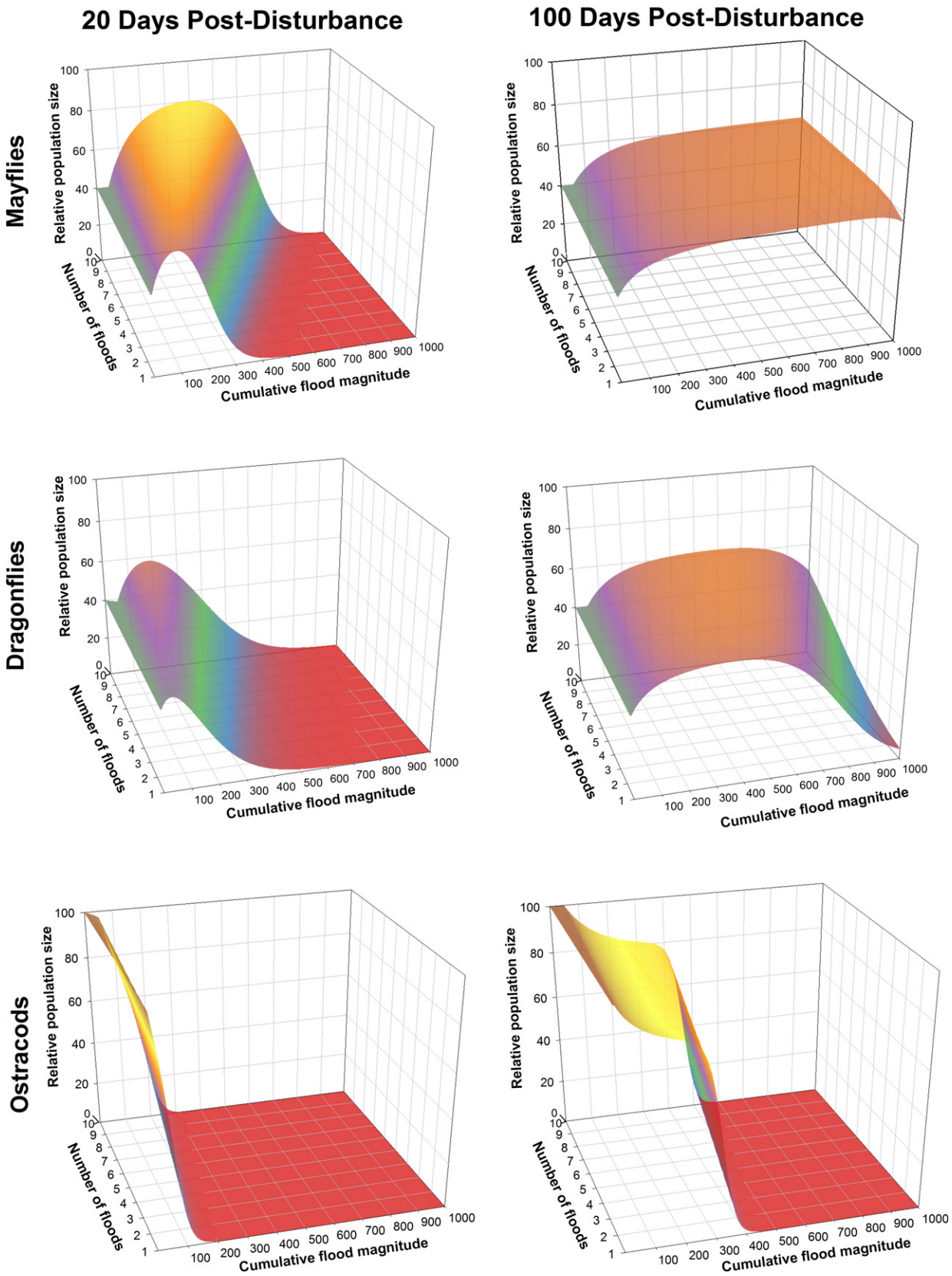

Figure 3 Relationship between flood frequency and cumulative flood magnitude for mayflies, dragonflies and ostracods at 20 and 100 days post-flood. Cumulative flood magnitude represents the sum of all flood events, distributed across 1 to 10 individual flood events. Twenty days after the series of flood events both number of floods and cumulative flood magnitude had a large effect on relative population size, while after 100 days the effects were more homogeneous.

Table 2 Flooding scenario model predictions and observed averages and standard errors for relative population size of: M – mayflies (*Fallceon quilleri*), D – dragonflies (*Progomphus borealis*) and O – ostracods (Ostracoda) after three prescribed flood events on the Bill Williams River, Arizona. Sites: A – below Alamo Dam; R – Rankin Ranch; M – Mineral Wash confluence.

			Model prediction			Observed relative population size (mean ± SE)		
Flood magnitude (cms)	Days post-flood	Site	M	D	O	M	D	O
68.8	21–23	A	56	–	20	66 ± 43	–	9 ± 9
		R	59	12	–	52 ± 23	17 ± 13	–
		M	56	17	17	44 ± 13	3 ± 2*	0*
29.2	1–2	A	9	–	6	10 ± 3	–	43 ± 20
		R	18	41	53	9 ± 5	29 ± 17	9 ± 6
		M	34	8	13	4 ± 1*	5 ± 3	37 ± 12
	12–13	A	38	–	27	29 ± 19	–	50 ± 22
		R	44	46	53	16 ± 4*	62 ± 13	4 ± 2*
		M	49	15	45	12 ± 3*	14 ± 4	17 ± 11
64.85	1–3	A	0	–	1	0 ± 0	–	3 ± 1
		R	5	22	0	4 ± 1	6 ± 3*	1 ± 1
		M	18	8	0	23 ± 7	19 ± 5	1 ± 1
	16	A	9	–	9	0 ± 0*	–	3 ± 1*
		R	43	38	4	11 ± 2*	5 ± 2*	0 ± 0*
		M	53	18	1	6 ± 3*	41 ± 33	2 ± 1
	33–34	A	51	–	54	0 ± 0*	–	3 ± 1*
		R	56	51	39	28 ± 4*	13 ± 5*	14 ± 11
		M	57	36	13	63 ± 20	34 ± 14	0 ± 0*

Note Values were rounded to the nearest integer.
*Cases where the model prediction did not fall within the 95% confidence interval of the observed relative population size.

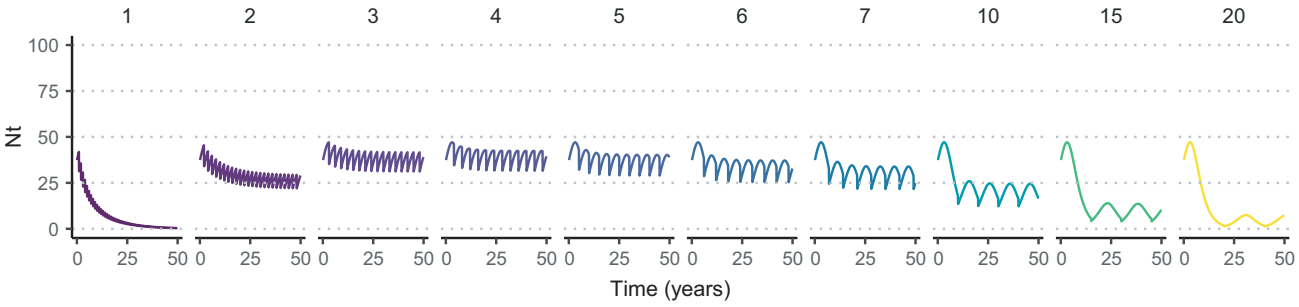

Figure 4 Relationship between fire return interval (ranging from 1 to 20 years) and relative population size (N_t) for a tropical savanna grass. The highest average population sizes were attained at return intervals of 3 to 4 years.

dragonflies, where predictions fell outside the 95% confidence intervals in only four cases. The model was least successful at predicting fast life-cycle mayfly numbers. Floods of a given magnitude may cause greater mortality on these taxa than expected under the model assumptions, and it is also possible that recovery after flood events may be slower than the trajectory of modelled population growth, especially in rivers where temperature or food resources are highly variable. An alternative explanation, however, is that the empirical data underestimated true population sizes. In a meta-analysis of multiple flood studies, McMullen & Lytle (2012) found that aquatic invertebrate abundances are often underestimated following flood events, possibly due to invertebrates remaining hidden in deep substrates difficult to sample following floods. The difference in model success among river sites shows that the model may need to be fine-tuned to particular habitats, and the difference in model success among years may be due to seasonality or climate effects.

Our study sheds light on the interaction between resistance (h) and resilience (r). In our characterisation of resistance and resilience, it appears that these traits in combination have a near-binary effect on population recovery, in contrast to finding a tradeoff between these two quantities (Miller & Chesson 2009; Nimmo *et al.* 2015). This is exhibited through certain combinations of r–h values allowing populations to recover to carrying capacity within a specified timeframe, and other combinations not allowing populations to recover within that timeframe. These findings suggest a binary relationship between resistance and resilience traits instead of a continuous relationship, and point to the existence of two distinct life-history syndromes – disturbance adapted vs. not disturbance adapted. Ostracods, which often inhabit non-flooding habitats such as ponds, may fall into the group of species whose combination of r–h values does not allow the population to recover readily after severe flood events. Other aquatic invertebrate taxa that are favoured during low-flow conditions may

fall into this group as well (Sponseller *et al.* 2010). Crook *et al.* (2010) found a positive correlation between resistance and resilience in freshwater fish in a study examining drought, indicating that while some species may be very poor at responding to drought, others may thrive, which agrees with our finding of two distinct life-history syndromes. The threshold-like reaction to disturbance events that we observed in the model indicates that it is important to examine the qualities of resistance and resilience simultaneously, making predictions based on both factors. Because of this relationship, knowledge of a species' resistance and resilience traits in relation to disturbance events may allow determination of whether their populations will respond favourably or not to these events.

Application of the model to a fire-driven savanna ecosystem revealed that intermediate fire return intervals on the order of 3 to 4 years produced the greatest population sizes, although the fire cycle itself caused considerable population variability due to mortality from fire, reduction in carrying capacity, and subsequent recovery. The population crash during the annual fire regime contrasts with that found by Silva *et al.* (1991), which found a critical fire frequency of 0.85 for the species to persist. That is, under their scenario, fire is required at minimum every 1.2 years for this species to persist. The discrepancy may be attributable to parameters estimates rather than model structure. The variable r in the logistic growth model is the intrinsic rate of population increase, which is essentially the maximum growth rate that a population can achieve under ideal conditions. This value may differ considerably from realised values of r obtained under field conditions with factors that hinder population growth (limited food, predation, temperature, etc.). The value of r we used in the fire example may be an underestimate for the reasons noted above, thus contributing to the discrepancy. Furthermore, we used a single value for fire intensity in our model projection, but fire intensity could be lower with shorter return times due to lower fuel loads (Silva & Castro 1989). Although we could not find specific values from the literature to parameterise the model for different fire intensities, halving disturbance intensities at the 1-year return interval resulted in population persistence under that scenario, which is congruent with Silva *et al.* (1991).

Management applications

There is a strong need to produce scientific models that can predict the outcome of alternative management outcomes (Walters 1997). In the case of disturbance regime management, an important management question is the allocation of effort to frequent, smaller disturbance events vs. fewer, larger events. The modelling framework is clearly useful for addressing that issue. Invasive species are also one of the primary threats to ecosystems worldwide. While prescribed disturbances could be used to favour native over non-native taxa, few attempts have been made to model the population-level consequences of these disturbance regimes for a diverse array of affected taxa. A modelling approach such as ours could be used to design disturbance regimes that achieve a particular conservation goal, such as maximising population size for favoured or endangered species and minimising it for nuisance or invasive species.

ACKNOWLEDGEMENTS

Funding was provided by a U.S. Department of Defense grant (SERDP RC-2511) and a U.S. Fish & Wildlife Service grant to D.A.L., a U.S. National Science Foundation grant (DMS-1411853) to P.D. and a U.S. National Science Foundation Predoctoral Fellowship to L.E.M. Helpful comments that resulted in substantial improvement to this manuscript were provided by Kate Boersma, Michael Bogan, Deb Finn and four anonymous reviewers.

AUTHOR CONTRIBUTIONS

LEM and DAL designed and conducted the empirical study. LEM, PD, JDT and DAL developed the theory, analysed empirical data and wrote the manuscript.

REFERENCES

Andersen, D.C. & Shafroth, P.B. (2010). Beaver dams, hydrological thresholds, and controlled floods as a management tool in a desert riverine ecosystem, Bill Williams River, Arizona. *Ecohydrology*, 3, 325–338.

Bond, N.R., Balcombe, S.R., Crook, D.A., Marshall, J.C., Menke, N. & Lobegeiger, J.S. (2015). Fish population persistence in hydrologically variable landscapes. *Ecol. Appl.*, 25, 901–913.

Crook, D.A., Reich, P., Bond, N.R., McMaster, D., Koehn, J.D. & Lake, P.S. (2010). Using biological information to support proactive strategies for managing freshwater fish during drought. *Mar. Freshw. Res.*, 61, 379–387.

Death, R.G. (2010). Disturbance and riverine benthic communities: what has it contributed to general ecological theory? *River Res. Appl.*, 26, 15–25.

Effenberger, M., Sailer, G., Townsend, C.R. & Matthaei, C.D. (2006). Local disturbance history and habitat parameters influence the microdistribution of stream invertebrates. *Freshw. Biol.*, 51, 312–332.

Elderd, B.D. & Doak, D.F. (2006). Comparing the direct and community-mediated effects of disturbance on plant population dynamics: flooding, herbivory and *Mimulus guttatus*. *J. Ecol.*, 94, 656–669.

Elderd, B.D. & Nott, M.P. (2007). Hydrology, habitat change and population demography: an individual-based model for the endangered Cape Sable seaside sparrow. *J. Appl. Ecol.*, 45, 258–268.

Franco, M. & Silvertown, J. (2004). A comparative demography of plants based upon elasticities of vital rates. *Ecology*, 85, 531–538.

Gray, L.J. (1981). Species composition and life histories of aquatic insects in a lowland Sonoran Desert stream. *Am. Midl. Nat.*, 106, 229–242.

Gray, L.J. & Fisher, S.G. (1981). Postflood recolonization pathways of macroinvertebrates in a lowland Sonoran Desert stream. *Am. Midl. Nat.*, 106, 249–257.

Grimm, N.B. & Fisher, S.G. (1989). Stability of periphyton and macroinvertebrates to disturbance by flash floods in a desert stream. *J. N. Am. Benthol. Soc.*, 8, 293–307.

Halpern, C.B. (1988). Early successional pathways and the resistance and resilience of forest communities. *Ecology*, 69, 1703–1715.

He, H.S. & Mladenoff, D.J. (1999). Spatially explicit and stochastic simulation of forest-landscape fire disturbance and succession. *Ecology*, 80(1), 81–99.

Hoffman, W.A., Adasme, R., Haridasan, M., de Carvalho, M.T., Geiger, E.L., Pereira, M.A.B. *et al.* (2009). Tree topkill, not mortality, governs the dynamics of savanna-forest boundaries under frequent fire in Central Brasil. *Ecology*, 90(5), 1326–1337.

Holomuzki, J.R. & Biggs, B.J.F. (2000). Taxon-specific responses to high-flow disturbance in streams: implications for population persistence. *J. N. Am. Benthol. Soc.*, 19, 670–679.

Junk, W.J., Bayley, P.B. & Sparks, R.E. (1989). The flood pulse concept in river-floodplain systems. In: *Proceedings of the International Large River Symposium* (ed. Dodge, D.P.). Canadian Special Publication of Fisheries and Aquatic Scientists, vol. 106, pp. 110–127.

Keith, D.A., Akcakaya, H.R., Thuiller, W., Midgley, G.F., Pearson, R.G., Phillips, S.J. *et al.* (2008). Predicting extinction risks under climate change: coupling stochastic population models with dynamic bioclimatic habitat models. *Biol. Let.*, 4, 5560–5563.

Lepori, F. & Hjerdt, N. (2006). Disturbance and aquatic biodiversity: reconciling contrasting views. *Bioscience*, 56, 809–818.

Lytle, D.A. (2001). Disturbance regimes and life history evolution. *Am. Nat.*, 157, 525–536.

Lytle, D.A. & Merritt, D.M. (2004). Hydrologic regimes and riparian forests: a structured population model for cottonwood. *Ecology*, 85, 2493–2503.

Lytle, D.A. & Poff, N.L. (2004). Adaptation to natural flow regimes. *Trends Ecol. Evol.*, 19, 94–100.

Lytle, D.A., Bogan, M.T. & Finn, D.S. (2007). Evolution of aquatic insect behaviours across a gradient of disturbance predictability. *Proc. R. Soc. B*, 275, 453–462.

Lytle, D.A., Olden, J.D. & McMullen, L.E. (2008). Drought-escape behaviors of aquatic insects may be adaptations to highly variable flow regimes characteristic of desert rivers. *Southwest. Nat.*, 53, 399–402.

Lytle, D.A., Merritt, D.M., Tonkin, J.D., Olden, J.D. & Reynolds, L.V. (2017). Linking river flow regimes to riparian plant guilds: a community-wide modeling approach. *Ecol. Appl.*, 27, 1338–1350.

Marchetti, M.P. & Moyle, P.B. (2001). Effects of flow regime on fish assemblages in a regulated California stream. *Ecol. Appl.*, 11, 530–539.

Marks, J.C., Power, M.E. & Parker, M.S. (2000). Flood disturbance, algal productivity, and interannual variation in food chain length. *Oikos*, 90, 20–27.

McMullen, L.E. & Lytle, D.A. (2012). Quantifying invertebrate resistance to floods: a global-scale meta-analysis. *Ecol. Appl.*, 22(8), 2164–2175.

Miller, A.D. & Chesson, P. (2009). Coexistence in disturbance-prone communities: how a resistance-resilience trade-off generates coexistence via the storage effect. *Am. Nat.*, 173, E30–E43.

Moyle, P.B. & Light, T. (1996). Biological invasions of fresh water: empirical rules and assembly theory. *Biol. Cons.*, 78, 149–161.

Nimmo, D.G., Mac Nally, R., Cunningham, S.C., Haslem, A. & Bennett, A.F. (2015). Vive la résistance: reviving resistance for 21st century conservation. *Trends Ecol. Evol.*, 30(9), 516–523.

Poff, N.L., Olden, J.D., Vieira, N.K.M., Finn, D.S., Simmons, M.P. & Kondratieff, B.C. (2006). Functional trait niches of North American lotic insects: traits-based ecological applications in light of phylogenetic relationships. *J. N. Am. Benthol. Soc.*, 25, 730–755.

Poff, N.L., Richter, B.D., Arthington, A.H., Bunn, S.E., Naiman, R.J., Kendy, E. *et al.* (2010). The ecological limits of hydrologic alteration (ELOHA): a new framework for developing regional environmental flow standards. *Freshw. Biol.*, 55, 147–170.

Power, M.E., Dietrich, W.E. & Finlay, J.C. (1996). Dams and downstream aquatic biodiversity: potential food web consequences of hydrologic and geomorphic change. *Environ. Manage.*, 20, 887–895.

Pyke, D.A., Brooks, M.L. & D'Antonio, C. (2010). Fire as a restoration tool: a decision framework for predicting the control or enhancement of plants using fire. *Restor. Ecol.*, 18(3), 274–284.

R Core Team (2015). *R: A Language and Environment for Statistical Computing*. R Foundation for Statistical Computing, Vienna, Austria. URL https://www.R-project.org/.

Richter, B.D., Mathews, R., Harrison, D.L. & Wigington, R. (2003). Ecologically sustainable water management: managing river flows for ecological integrity. *Ecol. Appl.*, 13, 206–224.

Richter, B.D., Warner, A.T., Meyer, J.L. & Lutz, K. (2006). A collaborative and adaptive process for developing environmental flow recommendations. *River Res. Appl.*, 22, 297–318.

Russell, R.E., Royle, J.A., Saab, V.A., Lehmkuhl, J.F., Block, W.M. & Sauer, J.R. (2009). Modeling the effects of environmental disturbance on wildlife communities: avian responses to prescribed fire. *Ecol. Appl.*, 19(5), 1253–1263.

Schleuning, M., Huaman, V. & Matthies, D. (2008). Flooding and canopy dynamics shape the demography of a clonal Amazon understorey herb. *J. Ecol.*, 96, 1045–1055.

Shafroth, P.B., Wilcox, A.C., Lytle, D.A., Hickey, J.T., Andersen, D.C., Beauchamp, V.B. *et al.* (2010). Ecosystem effects of environmental flows: modeling and experimental floods in a dryland river. *Freshw. Biol.*, 55, 68–85.

Shenton, W., Bond, N.R., Yen, J.D.L. & MacNally, R. (2012). Putting the "ecology" into environmental flows: ecological dynamics and demographic modelling. *Environ. Manage.*, 50, 1–10.

Silva, J.F. & Castro, F. (1989). Fire, growth and survivorship in a Neotropical savanna grass *Andropogon semiberbis* in Venezuela. *J. Trop. Ecol.*, 5, 387–400.

Silva, J.F., Raventos, J. & Caswell, H. (1990). Fire and fire exclusion effects on the growth and survival of two savanna grasses. *Acta Oecol.*, 11, 783.

Silva, J.F., Raventos, J., Caswell, H. & Trevisan, M.C. (1991). Population responses to fire in a tropical savanna grass, *Andropogon semiberbis*: a matrix model approach. *J. Ecol.*, 79, 345–355.

Smith, M., Caswell, H. & Mettler-Cherry, P. (2005). Stochastic flood and precipitation regimes and the population dynamics pf a threatened floodplain plant. *Ecol. Appl.*, 15(3), 1036–1052.

Sponseller, R.A., Grimm, N.B., Boulton, A.J. & Sabo, J.L. (2010). Responses of macroinvertebrate communities to long-term flow variability in a Sonoran Desert stream. *Glob. Change Biol.*, 16, 2891–2900.

Tonkin, J.D., Bogan, M.T., Bonada, N., Rios-Touma, B. & Lytle, D.A. (2017). Seasonality and predictability shape temporal species diversity. *Ecology*, 98, 1201–1216.

Townsend, C.R. & Hildrew, A.G. (1994). Species traits in relation to a habitat templet for river systems. *Freshw. Biol.*, 31(3), 265–275.

Walters, C. (1997). Challenges in adaptive management of riparian and coastal ecosystems. *Conservation Ecology [online]*, 1, 1.

Wolfram Research, Inc. (2015). Mathematica, Version 10.2. Wolfram Research, Inc., Champaign, IL.

Wootton, J.T., Parker, M.S. & Power, M.E. (1996). Effects of disturbance on river food webs. *Science*, 13, 1558–1561.

Yen, J.D.L., Bond, N.R., Shenton, W., Spring, D.A. & MacNally, R. (2013). Identifying effective water-management strategies in variable climates using population dynamics models. *J. Appl. Ecol.*, 50, 691–701.

SUPPORTING INFORMATION

Additional Supporting Information may be found online in the supporting information tab for this article.

Editor, Tim Wootton
Manuscript received 27 July 2017
Manuscript accepted 11 September 2017